How to read your LIDAR spec –
a comparison of single-laser-output and
multi-laser-output LIDAR instruments

Andreas Ullrich, Martin Pfennigbauer, Peter Rieger

RIEGL Laser Measurement Systems GmbH, February 2013

1   INTRODUCTION AND SUMMARY

Today's LIDAR marketplace offers a variety of airborne laser scanning (ALS) instruments with specification sheets that are often hard to read and apply in real-world applications. The purpose of an ALS system is to capture the topography of the ground in an effective way by means of a large number of measured coordinates. Often the metrics of the specsheets are given are in terms of scanning rates and maximum operating altitudes, but these alone do not provide insight into the real productivity and quality of data produced by each instrument. To alleviate this complexity, simple metrics for examining productivity and data quality are introduced. These metrics make it possible to more readily compare different ALS instruments.

Requirements for airborne LIDAR surveys specify point density in points (or measurements) per square meter. However, this metric of points per square meter does not provide information about the real quality of the data; the spatial point distribution on the target area. In other words the number of points measured on a surface is only relevant if the point pattern is uniform. A perfectly uniform point pattern will yield reliable sampling of the surface whereas an irregular point patter produces inconsistent sampling and therefore the data provides less information.

Additionally, the efficiency and productivity of ALS instruments is often assessed by the pulse repetition rate and scan speed of the system. While these metrics are helpful, they do not provide a complete picture of the productivity of a system. The fundamental metric for productivity and efficiency is fundamentally the total surface area the system can cover in a finite period of time.

These two metrics, coverage speed and data quality, have not been addressed thoroughly in the past. The focus of this paper is to provide a simple method of assessing ALS instruments through these methods and give an example comparison using real-world scenarios.

Specifically, this paper answers the following questions:

- How fast can LIDAR data be acquired while ensuring a specific point spacing on the ground?

- How does height variation of terrain impact acquisition speed?

- Can an instrument with a lower maximum measurement speed outperform instruments with higher measurement speeds with respect to total acquisition time?

When characterizing an ALS system, the interplay of the parameters of its subsystems, i.e. laser scanner (comprising a range finder and a scan mechanism), the INS, and the airborne platform, has to be carefully considered. In this paper we focus on the laser scanner, the LIDAR instrument. For the laser rangefinder we take the following parameters into account; laser pulse repetition rate and measurement rate, beam divergence, maximum range, and the capability to correctly resolve multiple time-around (MTA) echoes. For the scan mechanism we take into account the scan pattern, the field of view (FOV, i.e. the angular width of the scan

swath), and the scan speed (i.e. the number of scan lines per second, LPS, and the angular speed of the laser beam).

It is worth stressing that in order to assess the applicability of an instrument for a specific application, it is imperative to take into account all these parameters and their mutual impacts rather than singling out isolated alleged performance highlights. Limitations for single parameters may impose severe restrictions on the overall system performance and are sometimes not easily compensated for.

Section 2 prepares the way for comparing the performance of three different LIDAR instruments by (i) addressing the employed scan mechanisms, (ii) summarizing the key parameters of the instruments, (iii) explaining the technical terms *performance envelope* and *multiple-time around capability*, (iv) comparing the performance of the rangefinder subsystems of the LIDAR instruments, (v) discussing the performance of the scanner subsystem, the scan patterns, and (vi) deriving simple formulas for the optimum scan parameters to optimize point distribution on the ground. These considerations provide the basis for discussing point spacing and sampling frequency.

Sections 3 and 4 delve into the generation and analysis of LIDAR point clouds derived through simulation. The strategy and workflow of the simulation is described and results are presented for three different typical scenarios: corridor mapping, high density area mapping, and wide area mapping in mountainous terrain.

Section 5 discusses the importance of sampling frequency or point spacing in contrast to point density, especially with respect to object detection and object recognition.

The final chapter, 6, provides an analysis of the LIDAR instrument expressed as sampling frequency (point spacing) versus data acquisition speed. It demonstrates that a state-of-the-art single-channel 266,000-measurements-per-second LIDAR instrument outperforms a state-of-the-art dual-channel 500,000-measurements-per-second LIDAR instrument in any typical application and especially when acquiring data in hilly or mountainous terrain.

2 PREPARING THE PERFORMANCE COMPARISON

2.1 Scan Mechanisms

Today all major commercial topographic ALS instruments rely on one of the two following scan mechanisms:

- rotating multi-facet-mirror (i.e. polygon mirror)
- oscillating mirror

The clear advantage of using polygon mirrors is the continuous and smooth rotation of the mirror which leads to straight parallel scan lines on the ground (cf. Figure 1, a). The achievable scan rates are high and allow flexible adjustment for obtaining an even distribution of points on the ground. Furthermore, low vibrations and low stress on the deflecting mirror surfaces and the scan mechanism allow for maintaining constant and replicable measurement accuracy. The downside is that a certain fraction of the pulses produced by the laser do not result in measurement results as they never leave the instrument.

This is contrasted by oscillating mirrors where all laser pulses are available for LIDAR measurements. Taking the movement of the platform into account, the resulting scan pattern on a flat ground is typically triangular or sinusoidal, depending on how the oscillator mirror is driven by the electronics. In general, the measurements on the ground tend to concentrate near the turning points of the mirror (Figure 1, b). By employing sophisticated scan control hard- and firmware this can be alleviated but never entirely overcome.

There is an emerging class of instruments making use of a single scan mechanism but employing two or even more rangefinders – or at least laser beams – which have optical axes

slightly tilted with respect to each other (Figure 1, c). In these dual laser output instruments, each channel has its own scan pattern on the ground. By carefully selecting mission parameters it is possible to achieve a favorable interference pattern of the two scan patterns, at least in a flat terrain situation.
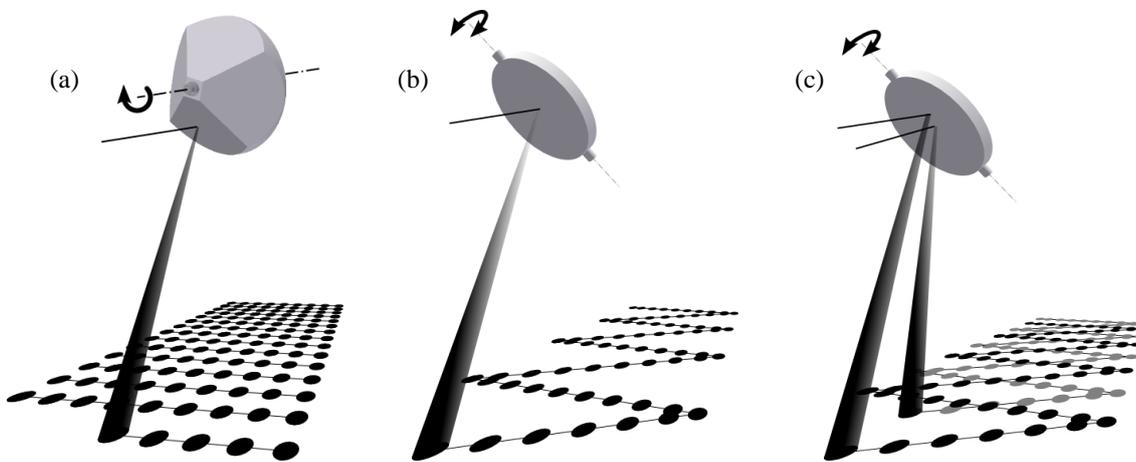

Figure 1: Principle of laser scanning mechanisms: rotating polygon wheel (a), single-channel oscillating mirror (b), and dual-channel oscillating mirror (c).

2.2 Instrument Parameters

We will evaluate and compare the performance of three state-of-the-art airborne laser scanning instruments:

- Instrument A with a rotating polygon mirror (i.e. the *RIEGL* LMS-Q780).
- Instrument B with a dual laser output and an oscillating mirror.
- Instrument C, another dual output laser instrument with an oscillating mirror.

In the following table, instrument parameters of instruments A, B, and C are listed [1][2].

	Instrument A	Instrument B	Instrument C
scan mechanism	rotating polygon	oscillating mirror	oscillating mirror
number of channels	single channel	dual laser output	dual laser output
flight altitude, AGL [1]	50 m - 3000 m	150 m - 3500 m	150 m – 5000 m
laser pulse rate	100 kHz - 400 kHz	2 x 40 kHz – 2 x 250 kHz	2 x 50 kHz – 2 x 250 kHz
measurement rate	66 kHz - 266 kHz	80 kHz - 500 kHz	100 kHz - 500 kHz
pulses in the air	up to 12	2 x up to 2	not disclosed
field of view	0 deg - 60 deg	0 deg - 75 deg	0 deg - 75 deg
scan rate	10 LPS – 200 LPS	0 LPS- 2 x 200 LPS	0 LPS- 2 x 280 LPS

[1] 10% target reflectance, 90% detection probability, 40 deg FOV, 23 km visibility

However, not all of the system parameters can be specified independently. In specific, there are two sets of parameters which are strongly related to each other:

- maximum permitted flight altitude (AGL), maximum laser pulse rate (measurement rate), and the capability of handling multiple pulses in the air,
- field of view and scan rate.

The first set of parameters is discussed below by means of the so-called performance envelope. The second set is subsequently discussed in more detail when deriving the optimum number of lines per second for specific flight parameters.

2.3   Operating Envelope

The performance envelope provides information on the maximum permitted pulse repetition rate for an intended flying height above ground. The performance envelopes displayed below are given for 40° FOV, 90% detection probability for 10% target reflectance, and 23 km visibility for the three instruments. The performance is directly related to the range finder of the LIDAR instrument and is thus given for a single channel for the dual channel instruments.

For example, instrument A can be operated up to 2300 m AGL at a laser pulse rate (PRR) of 400 kHz. At higher altitudes the pulse energy of the laser pulses is too low to provide ranging to 10% reflectance targets. By lowering the PRR, the energy per pulse increases and ranging is permitted up to 3500 m AGL at a PRR of 100 kHz.

The performance envelope clearly shows the benefit of handling a large number of pulses in the air simultaneously. This capability enables Instrument A to fully exploit its high potential of acquiring data *fast* from high altitudes. Additionally, instrument A is capable of acquiring data in different MTA zones within a single flight swath. In contrast, for Instrument B and C, proper flight planning must ensure that all targets within a single scan line of a swath will safely remain in one single MTA zone (compare Figure 3 below).
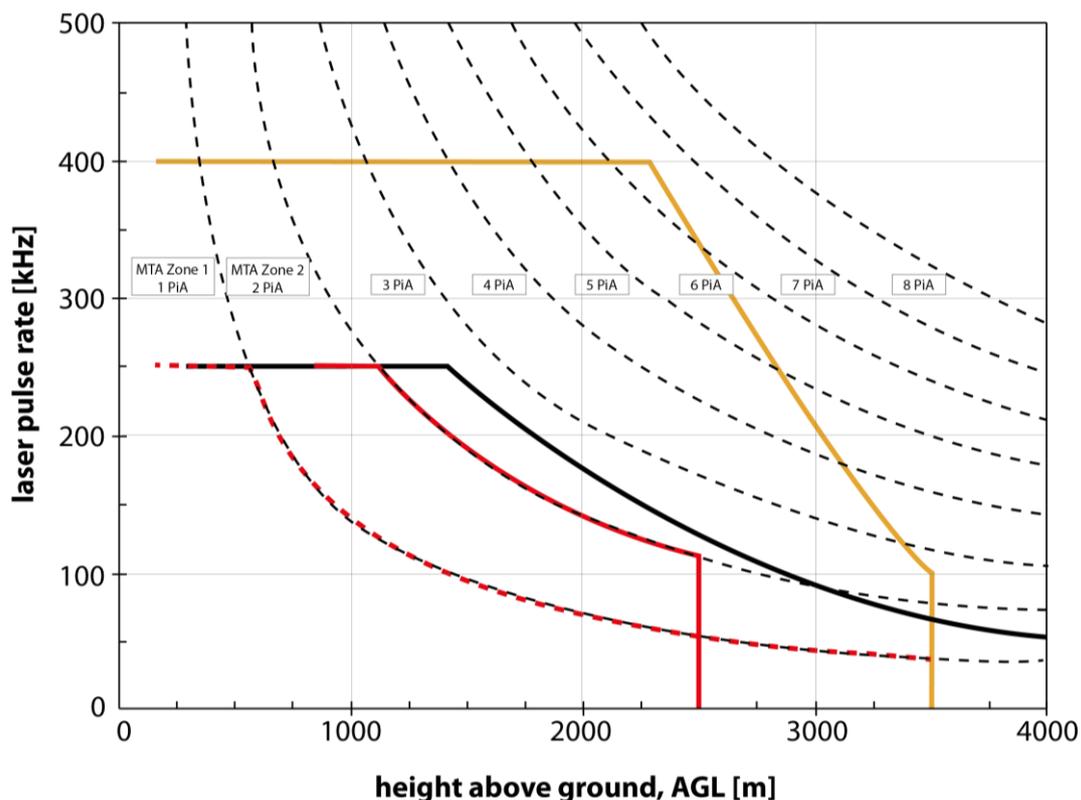

Figure 2: Performance envelope provided by the three instruments (per channel). Colors/styles used: orange Instrument A, red dashed Instrument B with just one pulse in the air, red solid Instrument B with 2 pulses in the air, black solid Instrument C. Dashed black lines indicate the borders of MTA zones.

Information contained herein is believed to be accurate and reliable. However, no responsibility is assumed by *RIEGL* for its use.
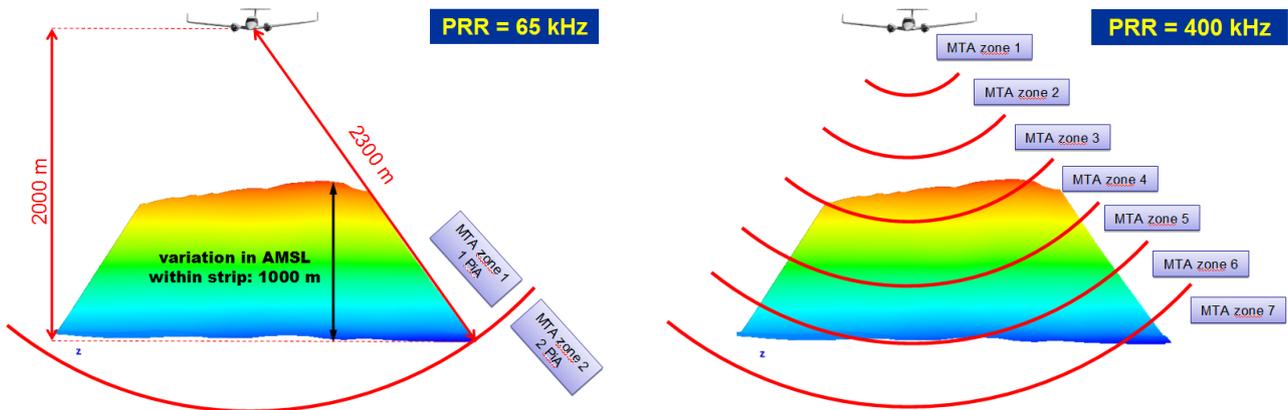
© Copyright *RIEGL* LMS
page 4 of 21

Figure 3: Illustrating multiple pulses in the air and its impact on the maximum permitted laser pulse repetition rate. Left hand side: in order to ensure that all targets of flight swath over mountainous terrain with 1000 m height variation remain in a single MTA zone, the PRR must be limited to 65 kHz. Right hand side: Instrument A can acquire data simultaneously in more than one MTA zone. In the example shown, data are acquired in zones 3 through 7.

2.4   Scanner Performance

Depending on the scan mechanism, there is a considerable interrelation between the field of view (FOV) and the number of scan lines per second. Additionally, as dual laser output systems make use of a single deflecting mirror, interference effects of the scan pattern has to be considered with respect to the achievable point spacing on the ground.

For the further discussion on the scanner performance we count a single scan line when the measuring beam moves from one edge of the swath to the other edge of the swath. Again, we consider at first a single channel of the dual channel instruments and deal with the interference aspect later.

The figure below shows the dependencies of the maximum number of lines per second (maxLPS) and the maximum angular speed of the measuring beam (max$\partial\alpha/\partial$t) versus the field of view for the different instruments according to published specifications. It is worth noting that for Instrument A, both maxLPS and max$\partial\alpha/\partial$t are independent of FOV and high compared to the two other instruments at high FOV values.
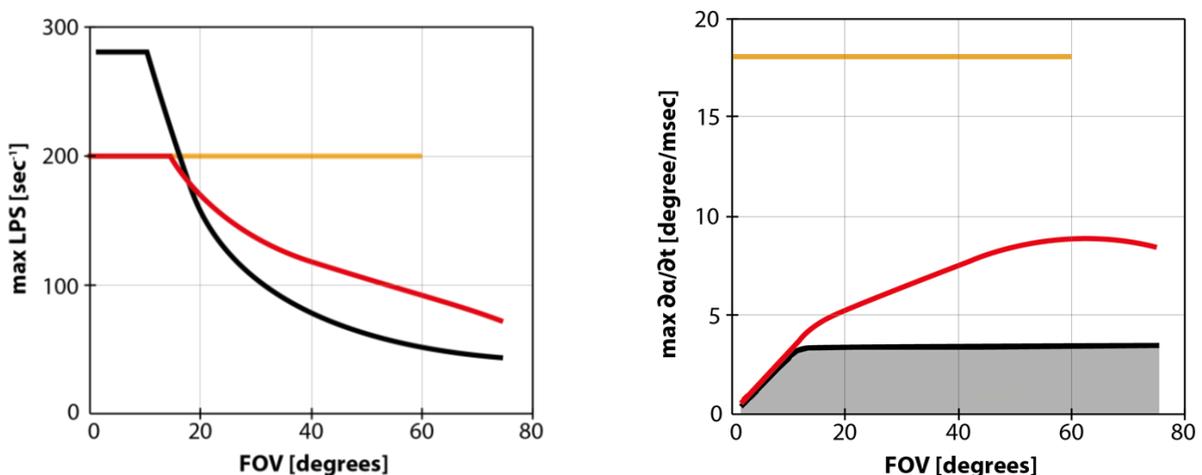

Figure 4: Left hand side: maximum number of lines per second (for a single channel) versus field of view (FOV) for Instrument A (orange), Instrument B with a sinusoidal scan pattern (red) and Instrument C with a triangular scan pattern (black). Right hand side: maximum angular speed of the laser beam versus FOV. Same coloring scheme used. The grey area indicates the possible choices of angular scan speed and FOV for Instrument C.

The number of lines per second translates directly into line spacing on the ground, and angular scan speed translates into point spacing within a scan line as displayed in Figure 5. Given the speed above ground (v) of the LIDAR instrument, the line spacing b is simply $b=v/LPS$. The angular spacing between laser shots is simply $\partial\alpha/\partial t$ / *PRR* and the point spacing a on the ground for a given slant range R is $a=R\partial\alpha/\partial t$ / PRR (paraxial approximation).

In order to have non-overlapping laser footprints on the ground, Instrument B with a 1/e² beam divergence of 0.35 mrad would require a minimum angular speed of 5 degrees per millisecond for a PRR of 250 kHz (its maximum pulse repetition rate), but is capable of providing 3 deg/msec maximum. Thus Instrument B cannot provide non-overlapping footprints at the maximum PRR.

The high number of lines per second at low FOV appears favorable for some special applications. Unfortunately they do not translate into a high angular speed at low FOV as the mirror must stop at the edge of the FOV before accelerating into the opposite direction for each line. In the region where this reversed acceleration occurs, separating footprints on the ground becomes exceptionally complex.

In most LIDAR applications the terrain must be sampled (discussion on sampling the terrain later on) with a maximum permitted point spacing on the ground. Therefore, it is common practice to try adjusting all parameters (AGL, speed above ground, PRR, LPS) in a way that the line spacing and the point spacing within the line become equal. Scan patterns are displayed in Figure 6 together with the equations for the optimum number of lines per second for each instrument. For the matrix scan pattern of Instrument A and the triangular scan pattern of Instrument C, the spacing a, at the edges of the swath must equal b, in the center of the swath. Whereas for the sinusoidal pattern of Instrument B, the spacing a is also taken at the center of the swath. For this calculation we already consider the optimum interference of the two scan patterns on the ground from the two channels of Instruments B and C, filling up the gaps at the edges of the swaths. Note that for the scan pattern of a single channel the line distance at the edges is *2b*. Please note that due to the low maximum scan speed of the oscillating mirror scanner for high FOVs, the optimum number of LPS according to the equations cannot be achieved for some parameter sets.
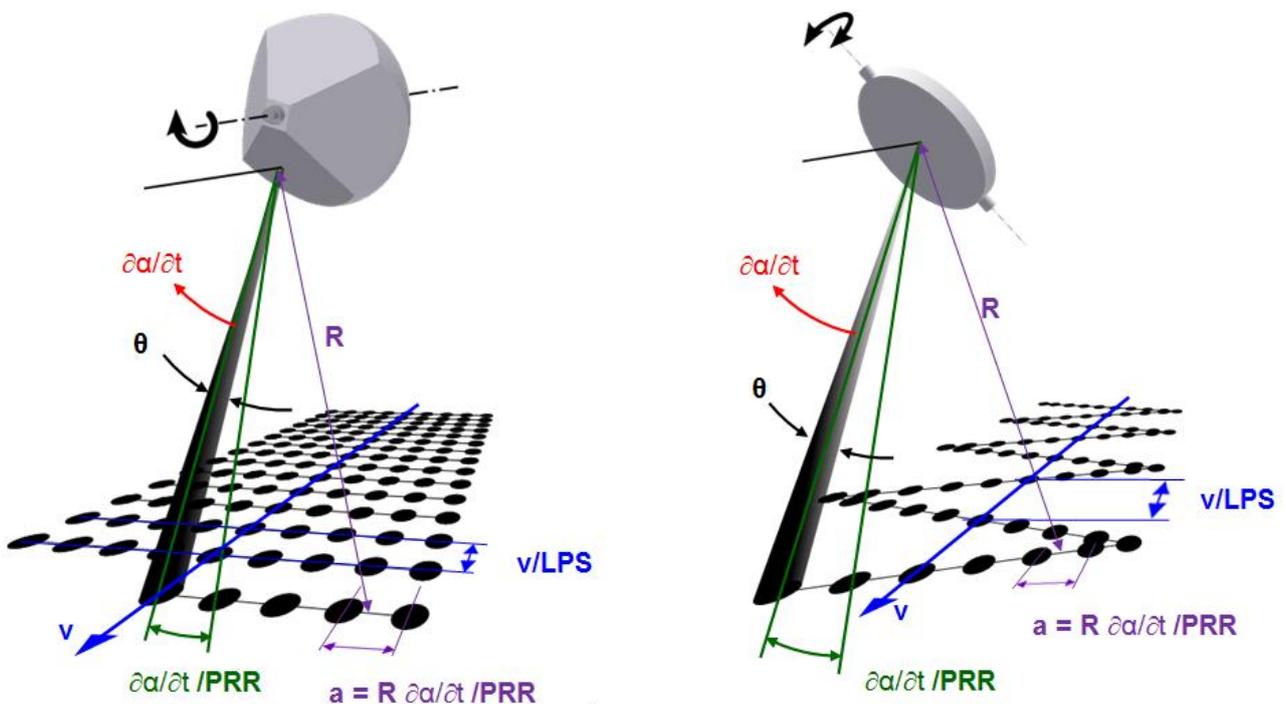

Figure 5: Point spacing within a scan line, *a*, and line spacing, *b*, on the ground for the polygon mirror scanner (left) and the oscillating mirror scanner (right). v ... speed of platform, LPS ... lines per second, PRR ... laser pulse repetition rate, $\partial\alpha/\partial t$ ... angular speed of the measurement beam, θ ... beam divergence, R ... slant range.

Left side patterns A, B, C. Right side equations:

$$LPS_{optimum} = \cos\left(\frac{FOV}{2}\right)\sqrt{\frac{2}{\pi}}\sqrt{\frac{v.PRR}{AGL}}$$

$$LPS_{optimum} = \sqrt{\frac{2}{\pi.FOV}}\sqrt{\frac{v.PRR}{AGL}}$$

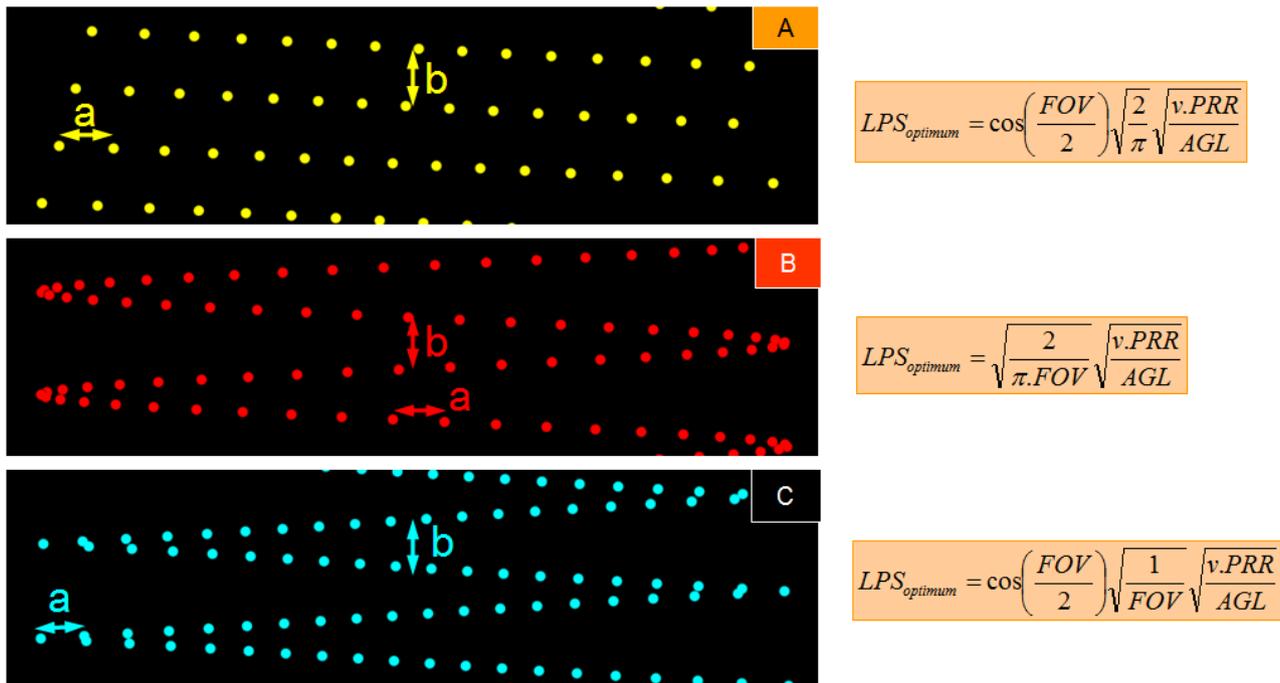$$LPS_{optimum} = \cos\left(\frac{FOV}{2}\right)\sqrt{\frac{1}{FOV}}\sqrt{\frac{v.PRR}{AGL}}$$

Figure 6: Left hand side: Scan pattern for Instrument A (top), and a single channel of Instruments B and C (middle and bottom) for illustration. Right hand side: equations for the optimum choice of the number of lines per second. The equation for Instrument A is valid for a polygon mirror with four facets.

The dual channel instruments perform range measurements in slightly different directions at the same time. As both channels are deflected by a single oscillating mirror, the two beams will be separated angularly in flight direction. Each channel generates its own scan pattern on the ground and it is the intention to have a favorable interference of the two scan patterns as sketched in the figure below. The actual phase between the two scan patterns depends on the speed above ground, the height above ground, and the number of lines per second. For flat terrain, active control loops can ensure the favorable out-of-phase condition, whereas for mountainous terrain or even for hilly terrain, the phase condition cannot be maintained over the whole terrain and the favorable interference will develop into the unfavorable without the possibility of any counter measures.

Information contained herein is believed to be accurate and reliable.
However, no responsibility is assumed by *RIEGL* for its use.
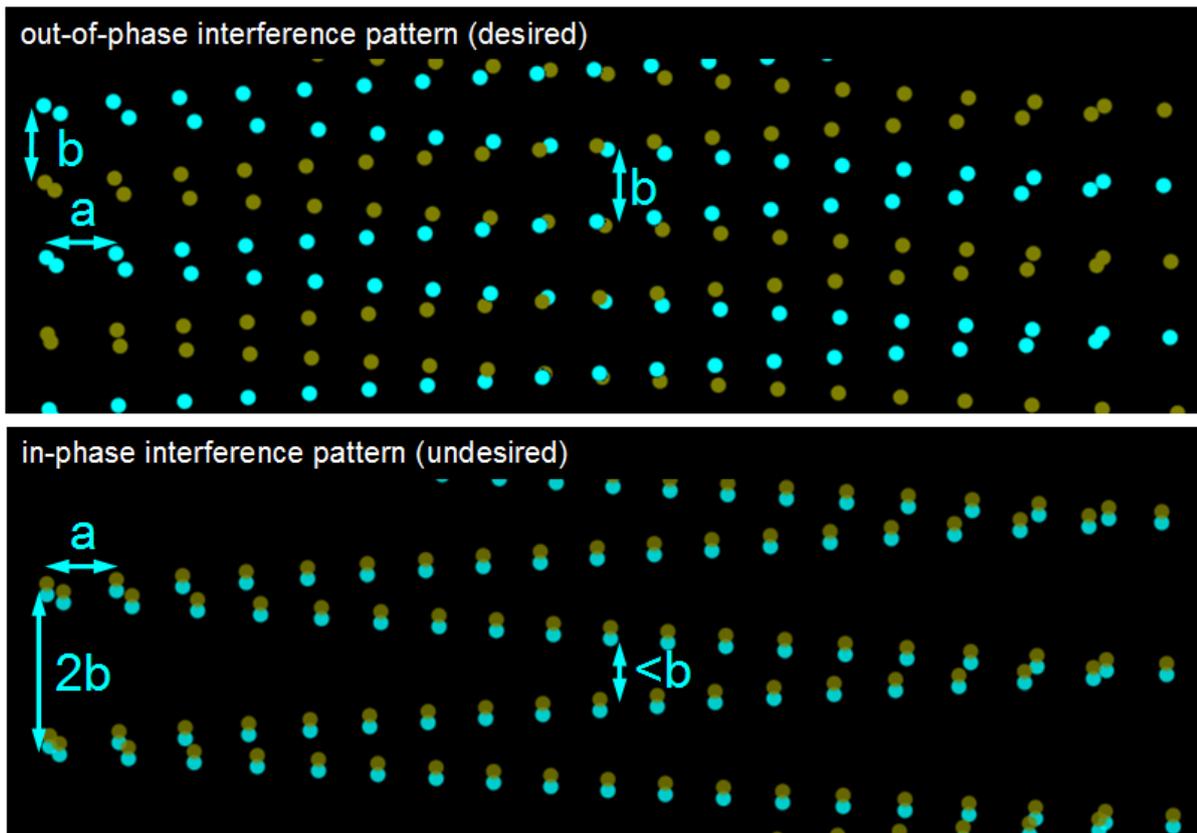
© Copyright *RIEGL* LMS
page 7 of 21

Figure 7: Interference patterns of a dual laser output system. The scan patterns of the channels are shown in different colors. Top: the favorable out-of-phase interference pattern. Bottom: the unfavorable in-phase interference pattern with *2b* line spacing at the edges.

2.5   Point Spacing and Point Density

LIDAR data is acquired sequentially, i.e., measurement by measurement in single laser output LIDAR instruments and two measurements at a time in dual laser output instruments. In any case, when addressing point spacing, it is convenient to organize the actual measurements into scan lines. The whole scan pattern is then composed of a large number of scan lines. The measurements on the target surface have a spacing along the scan lines, denoted *a*. The scan lines themselves have a specific spacing between each other, denoted as *b*. The distance of consecutive scan lines along the flight direction varies significantly over the swath width for oscillating scan mirrors, especially near the edges of the swath (compare also the sketches in the previous subsection).

It is common practice to base the flight / mission planning on either the nominal point spacing (NPS) or on the point density, usually measured in points per square meter (or similar points / measurement per area metrics). The "LIDAR Guidelines and Base Specification", [3] states the term "nominal point spacing" without giving a rigorous definition of the term. The draft version of the ASPRS standard "LIDAR density and spacing specification", [4], defines two metrics; the LDSS point spacing and the LDSS point density as statistical metrics for post-acquisition and post-processing quality control of ALS point clouds.

For the subsequent considerations, in deviation from the ASPRS a posterior metric point spacing, we use the worst case nominal point spacing as the maximum of all edges connected to a point instead of using the average value. This ensures that gaps in the sampling of the ground are accounted for in their worst case and are not reduced by very dense or even overlapping measurements within a single scan line.
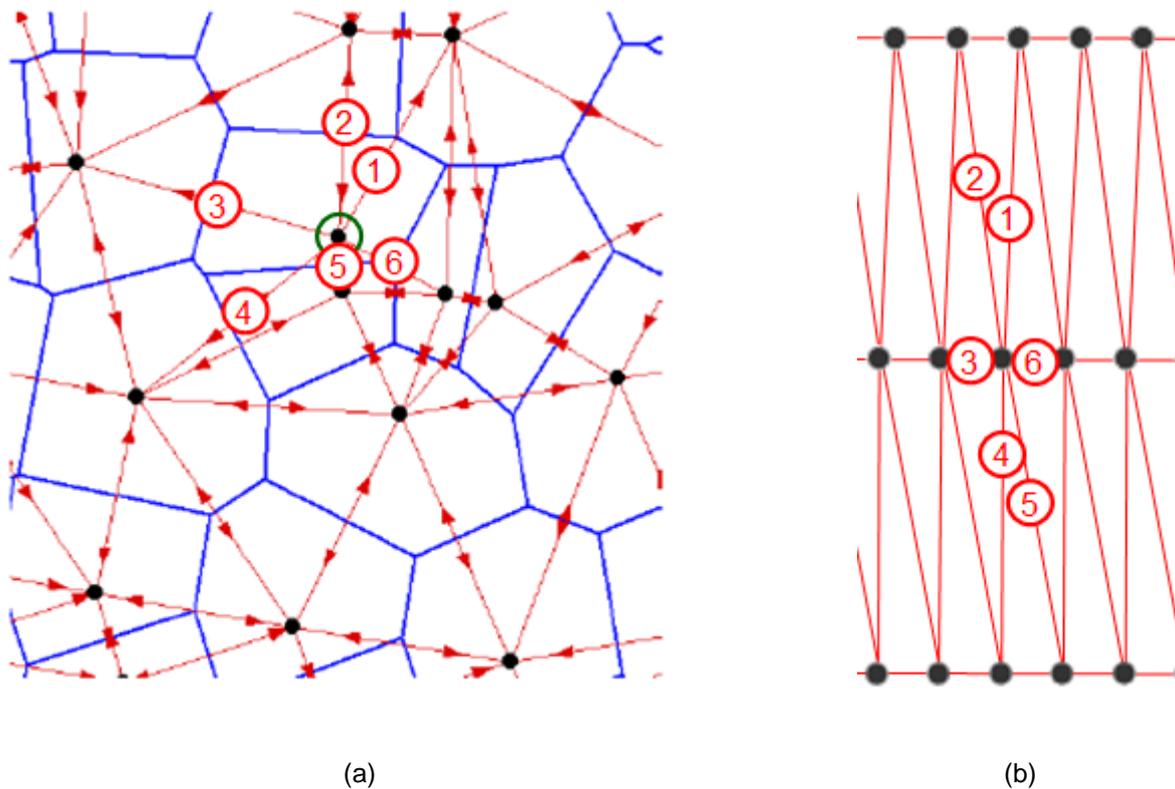
(a) (b)

Figure 8: Each black dot represents a measurement on the ground. Red lines are the edges of triangles according to a Delaunay triangulation. Blue polylines indicate Voronoi cells. (a): Irregularly distributed points. The example is taken from [5]. (b): Regular scan pattern with longer spacing between scan lines and shorter spacing along the scan lines.

To provide symmetry we will make use of the inverse of the nominal point spacing (1/NPS) to have a metric similar to the point density, which is usually given in points/m². Therefore the two metrics are:

- Nominal sampling frequency, measured in points per meter, which is the inverse of the NPS. E.g., a sampling frequency of 2 points/m corresponds to a nominal point spacing of 0.5 m.

- Nominal point density, measured in points per square meter, i.e., the number of points within some test region, divided by the area of that region.

As it will be demonstrated further on, it is the nominal sampling frequency that actually counts when it comes to object detection, surface reconstruction, modeling and much more.

3   LIDAR POINT CLOUDS FROM SIMULATION

In order to compare the performance achievable with the three different instruments, simple mathematical models for each of the instruments have been derived and the instruments have been "flown" over terrain models at their optimum parameters. The figure below shows the work flow on the left hand side, and the interdependencies on the right hand side.
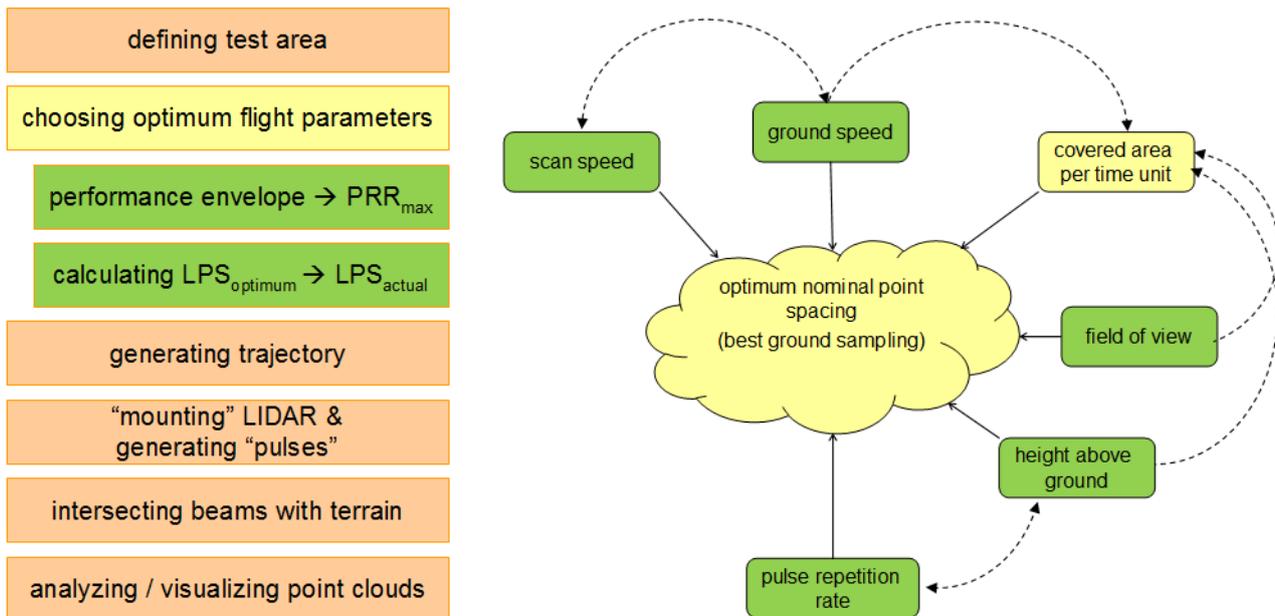

Figure 9: Left: Workflow for simulating representative point clouds. Right: Interdependencies of parameters influencing acquisition speed and sampling frequency (inverse of nominal point spacing).

The initial step is defining the test area and thus the height variation of the terrain. For the terrain, NASA SRTM data have been used. The optimum flight parameters are selected in order to achieve the highest acquisition speed, i.e., the highest covered area per time unit, usually km²/h, while maintaining the highest ground sampling frequency, i.e., the smallest nominal point spacing. However, both metrics are influenced by parameters such as speed over ground, field of view, height above ground, laser pulse repetition rate and scan speed, and the limitations imposed on these parameters by the specific instrument. The next steps are to generate the trajectory according to the selected AGL, mount the LIDAR on a virtual aircraft cruising with the selected speed above ground, generate the pulses, i.e., measurement beams in space and intersect them with the terrain model. This results in a point cloud which is further used for analysis and visualization.

Information contained herein is believed to be accurate and reliable.
However, no responsibility is assumed by *RIEGL* for its use.

© Copyright *RIEGL* LMS
page 10 of 21

4   PERFORMANCE COMPARISON

Subsequently the point density, point spacing, and point distribution under typical surveying conditions are investigated for different scenarios and the three instruments. The table below summarizes the key parameters.

	scenario 1	**scenario 2**	**scenario 3**
application	corridor mapping	high density survey	wide area mapping
terrain	flat	flat	mountainous
AGL	500 m	1000 m	1000 m – 2000 m
speed	60 kn	120 kn	140 kn
FOV	60 deg	60 deg	60 deg

Scenario 1 represents typical corridor mapping applications from a rotary wing aircraft with a typical speed of 60 kn and a 500 m (1500 ft) AGL flight path. Scenario 2 depicts typical high-density surveying from a single-engine fixed-wing aircraft and a 1000 m (3000 ft) AGL flight path. Scenario 3 deals with the most challenging data acquisition environment, a mountainous region with significant height variation within a single flight swath. Figure 10 provides a view of the terrain models used for the simulations; a flat region and a mountainous regions.
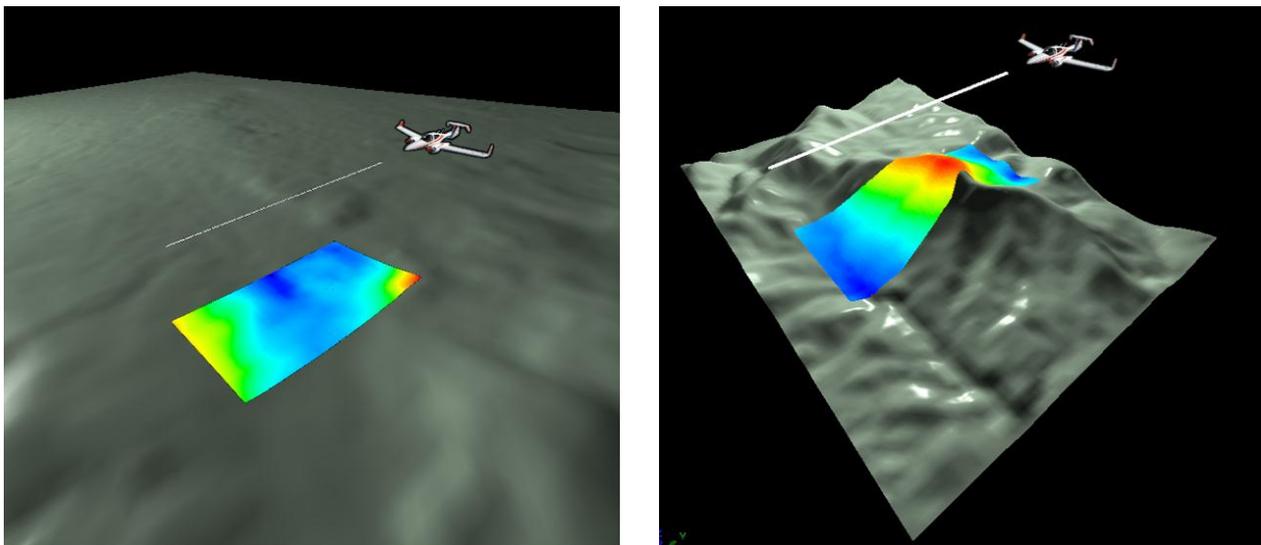

Figure 10:
Terrain models used for simulation. Height encoded point cloud of Instrument A overlaid.
Left: height variation of 60 m, used for scenarios 1 and 2.
Right: height variation of 1000 m within a single flight line, used for scenario 3.

4.1   Corridor Mapping

The corridor mapping application can be subdivided into two subcategories; Power Line Mapping and Area Mapping. In Power Line Mapping, the parameters of the instruments are usually set to achieve a dense sampling within the scan lines in order to map the wires of the power line. This is achieved by a low scan speed so that there are no gaps between consecutive laser footprints on each line.

The table below shows the operating parameters for the three instruments for Power Line Mapping. Figure 11 shows the actual distribution of the footprints according to the simulation. The size of each footprint is calculated from the specified beam divergence (if necessary converted to the 1/e²-value) and the slant range.

All three instruments can provide dense laser footprints within the lines without gaps. Instrument A provides the lowest (best) line spacing and thus the best sampling quality.

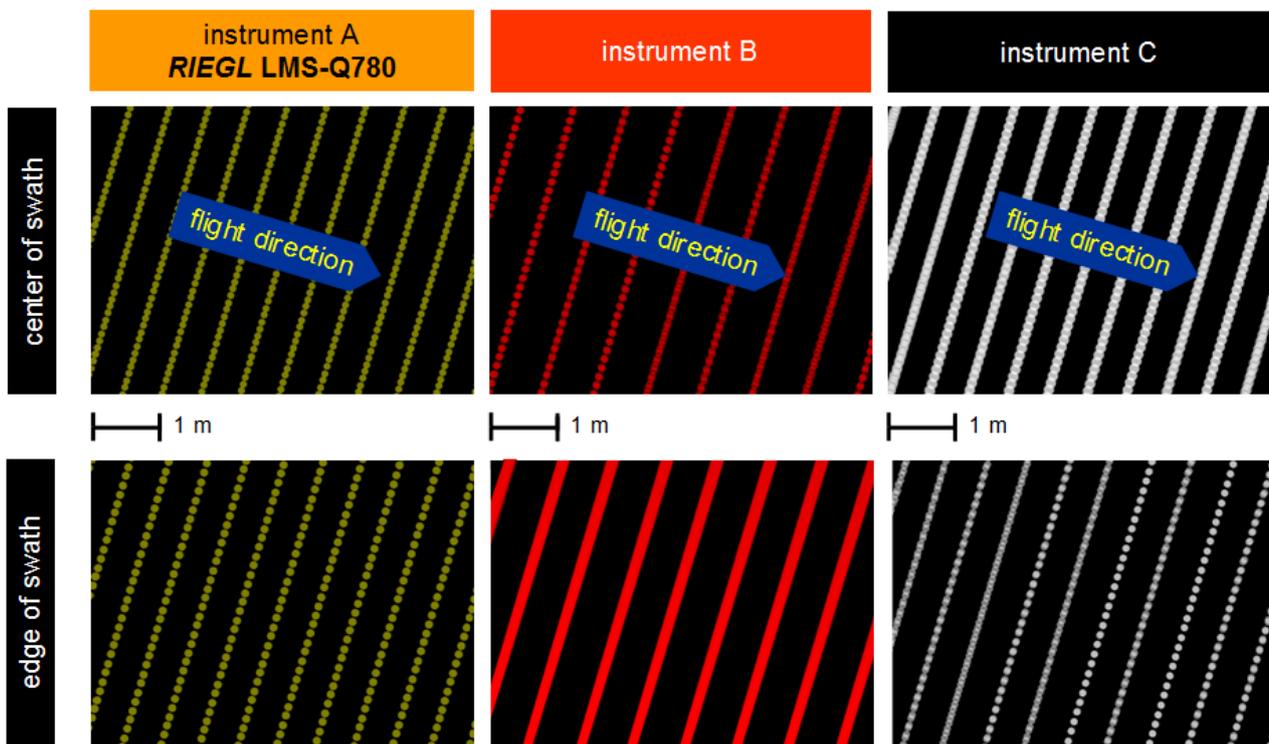|	AGL	FOV	measurement rate	LPS	point spacing a	line spacing b	avg. point density
Instrument A	500 m	60 deg	1x 266 kHz	1x 55 LPS	0.11 m	0.45 m	16.5 p/m²
Instrument B	500 m	60 deg	2x 245 kHz	2x 41 LPS	0.14 m	0.76 m	30.2 p/m²
Instrument C	500 m	60 deg	2x 244 kHz	2x 53 LPS	0.15 m	0.58 m	30.2 p/m²

Figure 11: Distribution of laser footprints for scenario 1; optimized for power line mapping.

For the second subcategory it is essential to distribute the laser footprints equally in both directions, along the flight direction and across the flight direction. Instrument A with its matrix scan pattern easily achieves this task, Instrument B achieves nearly the same sampling quality. For instrument C the flight height needs to be increased to cope with the limitation in scan speed. Point spacing is almost the same as for instrument A, however, an inspection of the footprints on the ground shows that the measurements are not independent as the footprints overlap significantly (compare Figure 12).

Information contained herein is believed to be accurate and reliable. However, no responsibility is assumed by *RIEGL* for its use.

© Copyright *RIEGL* LMS
page 12 of 21

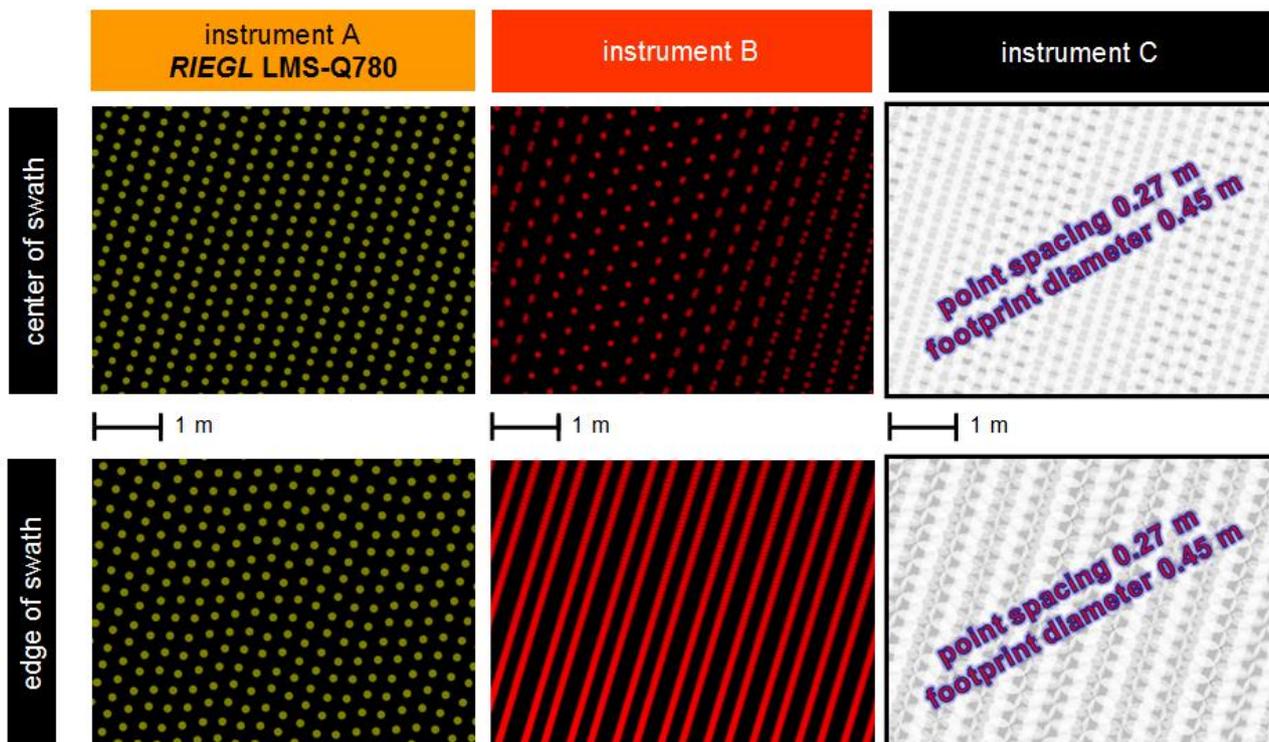|	AGL	FOV	measurement rate	LPS	point spacing a	line spacing b	avg. point density
instrument A	500 m	60 deg	1x 266 kHz	1x 109 LPS	0.28 m	0.28 m	16.5 p/m²
instrument B	500 m	60 deg	2x 245 kHz	2x 93 LPS	0.32 m	0.33 m	30.2 p/m²
instrument C	**1300 m**	**25 deg**	2x 250 kHz	2x 114 LPS	0.27 m	0.27 m	30.2 p/m²

Figure 12: Distribution of laser footprints for scenario 1 and optimized for area mapping.

4.2   High Density Large Area Survey

For the large area high-density survey from a fixed-wing aircraft 3000 ft above ground, the situation is quite similar compared to the area survey from 1500 ft. In order to achieve an equal distribution in both horizontal directions, Instrument C has to be operated from a higher altitude with a reduced FOV to achieve the required higher scan speed. Again Instrument A provides the best ground sampling, although capable of providing only 266 kHz of measurements on the ground compared to instrument B operating at 500 kHz of measurements. However, a lot of measurements are "wasted" at the edges and also in the overlapping regions near nadir by instrument B, not contributing to an improved ground sampling.

	AGL	FOV	measurement rate	LPS	point spacing *a*	line spacing *b*	avg. point density
instrument A	1000 m	60 deg	1x 266 kHz	1x 108 LPS	0.57 m	0.57 m	4.1 p/m²
instrument B	1000 m	60 deg	2x 250 kHz	2x 93 LPS	0.61 m	0.66 m	7.7 p/m²
instrument C	**1900 m**	**34deg**	**2x 180 kHz**	**2x 94 LPS**	**0.65 m**	**0.66 m**	**5.5 p/m²**

The figure below shows once more the distribution of the laser footprints on the ground. Flight direction is vertical. Note the slightly overlapping footprints delivered by instrument C.
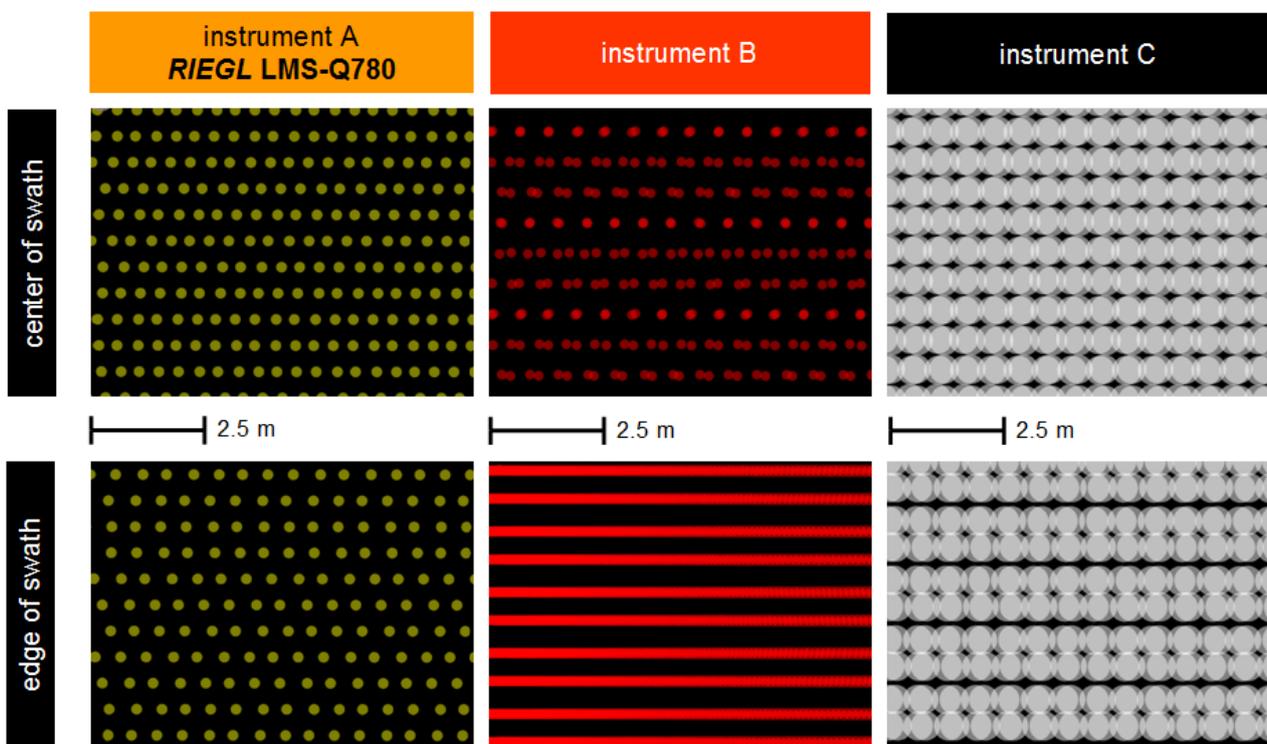

Figure 13: Distribution of laser footprints for scenario 2.

4.3   LIDAR Data Acquisition in Mountainous Areas

Acquiring LIDAR data in a mountainous region is, in general, a challenging task. According to the variation in terrain height, the swath width will vary too. A common approach in providing high density LIDAR data in mountainous regions is to work with rather small swath widths and to follow the terrain. However, this reduces the acquisition speed measured in km²/h drastically and thus makes the data acquisition considerably more expensive.

With Instrument A's ability to acquire data in different MTA zones during a single swath enables an alternative approach: flying high with a fixed wing aircraft. This yields the most time-efficient and cost efficient approach.

The subsequent simulation reflects this approach. Flying at AGL values between 1000 m and 2000 m above the terrain (1000 m height variation) without attempting to follow the ground produces point clouds with significantly different sampling qualities for the three instruments.

Mountainous terrain as well hilly terrain is especially challenging for dual laser output systems as the intended out-of-phase condition for the scan patterns of the two channels cannot be maintained due to the significant change in AGL in a single scan line.

Furthermore, the pulse repetition rate and thus the measurement rate of Instruments B and C have to be reduced significantly to ensure that all objects are within a single MTA zone.

The table below summarizes the achievable point spacing and Figure 14 gives the distributions of the laser footprints in nadir and at the swath edges. Note that for the swath edges two different distributions are displayed. The best case reflects the favorable out-of-phase interference, whereas the worst case reflects the unfavorable and unavoidable in-phase condition.

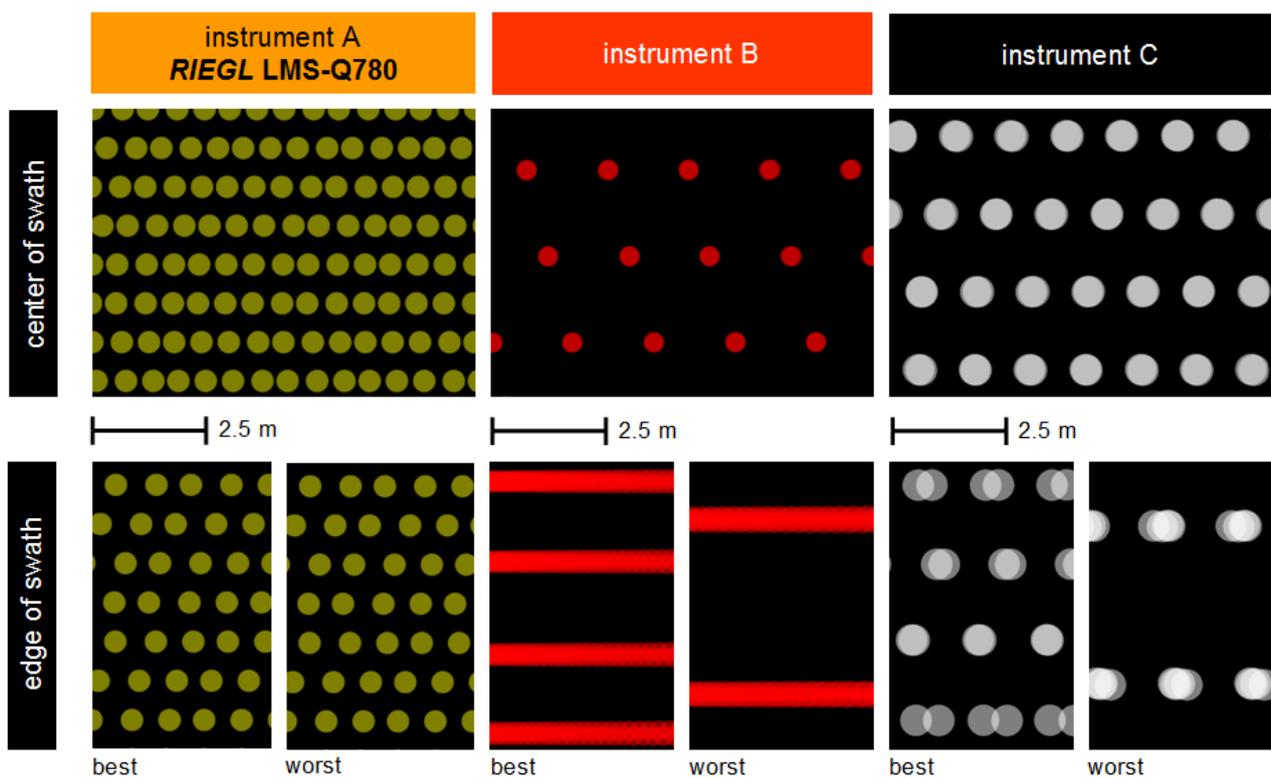|	AGL	FOV	measurement rate	LPS	point spacing a	line spacing b	avg. point density
Instrument A	2000 m	60 deg	1x 266 kHz	1x 83 LPS	0.87 m	0.87 m	1.3 - 3.5 p/m²
Instrument B	2000 m	60 deg	2x 63 kHz	2x 37 LPS	1.94 m	4.32 m	0.53 - 1.9 p/m²
Instrument C	2000 m	60 deg	2x 66 kHz	2x 41 LPS	1.74 m	3.50 m	0.9 - 2.6 p/m²

Figure 14: Distribution of laser footprints for scenario 3.

5   SAMPLING THE TERRAIN WITH LASER FOOTPRINTS

In order to demonstrate the crucial importance of the nominal point spacing and thus the sampling frequency of a specific scan pattern we placed an artificial object on the terrain in the mountainous region near the edge of the swaths generated for every instrument. To make the reader familiar with the display, a real example is shown in Figure 15 below showing a point cloud, color encoded by height, from a top view. Blue footprints hit the lower surroundings of a small house, whereas the red footprints are located on the roof. The object becomes more easily recognized when taking perspective views on the point cloud.

Figure 16 shows simulated point clouds from scenario 3 taken at the edges of the swaths. Color encoding is similar to the one used in the figure above: a laser footprint is colored blue when hitting a low target surface, red when it hits an elevated target surface. According to the sampling theorem, the sampling frequency must be at least twice the highest spatial frequency of the object to be sampled, in order to be able to reconstruct the object or at least to do an object recognition/detection routine. Even though the point density measured in points per square meter is more or less the same for all of the instruments.
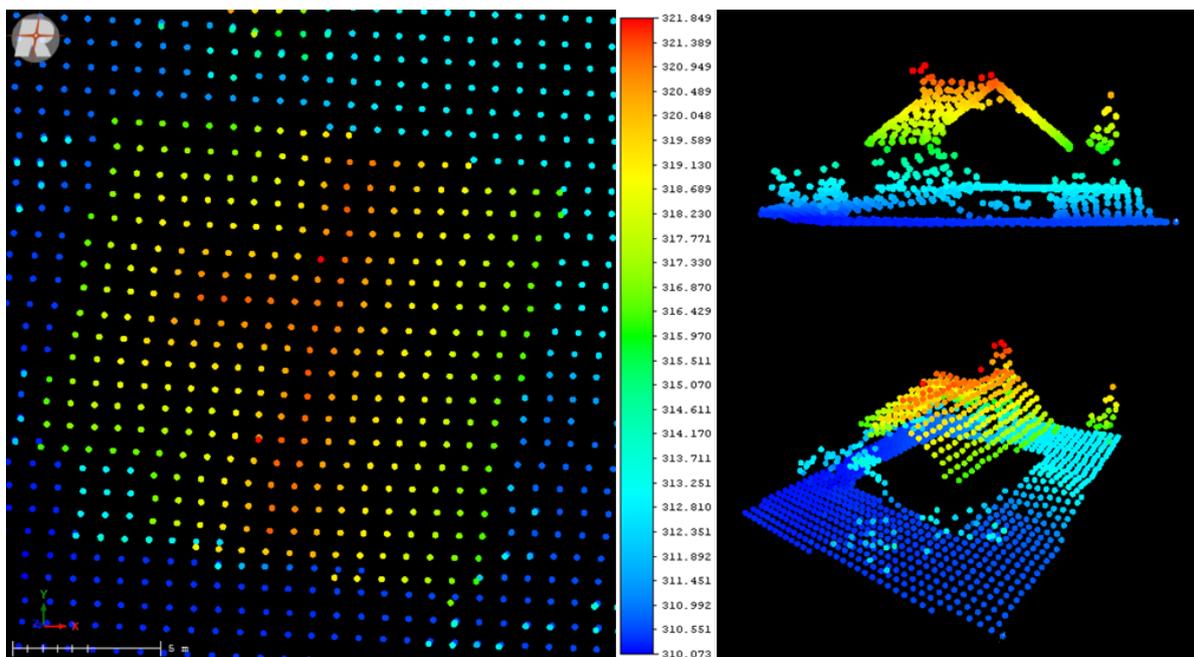

Figure 15: Real world example of an object sampled with Instrument A. Left: top view of point cloud, Color encoding according to height (blue .. low, red .. high). Right: perspective views of the same point cloud.
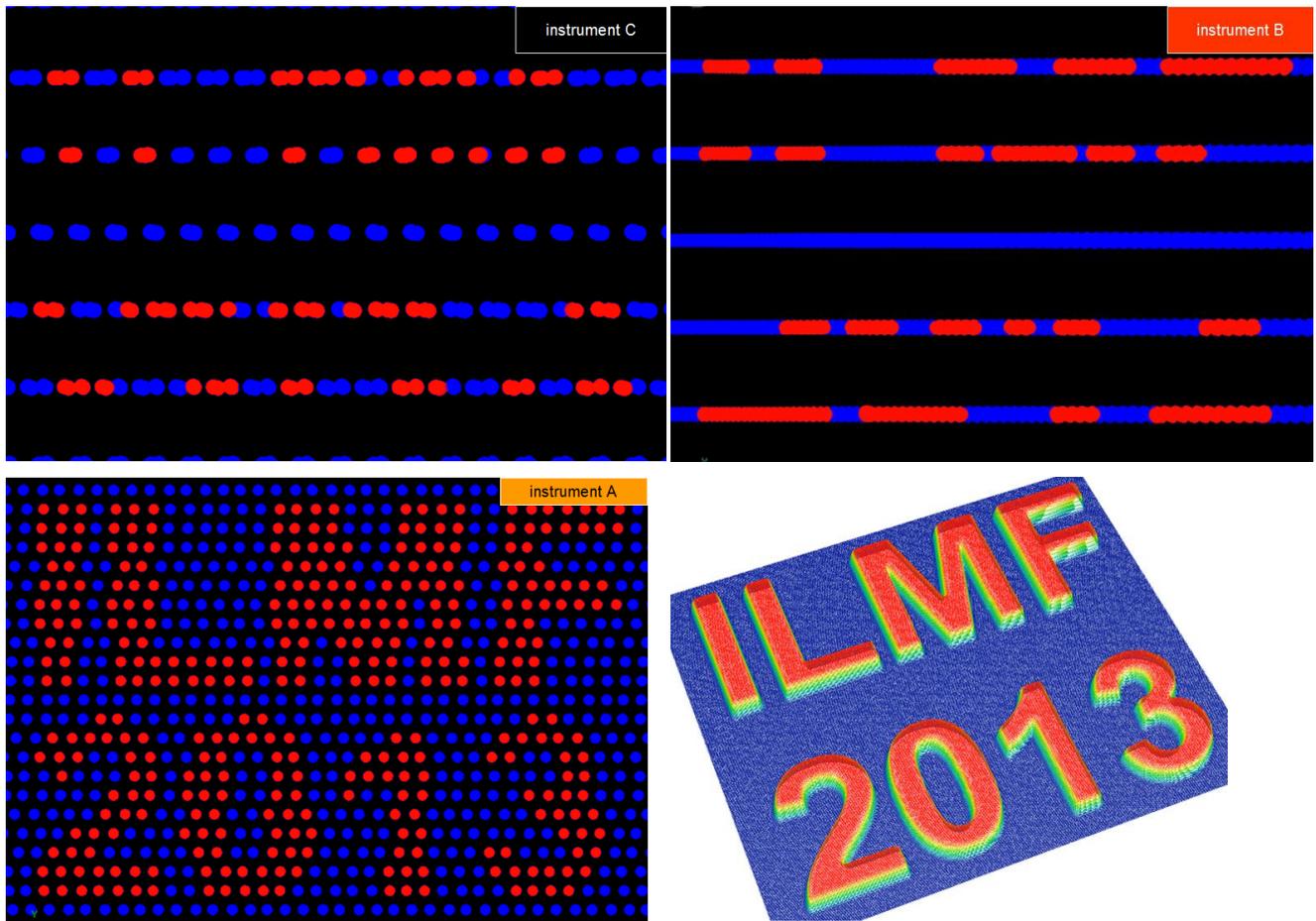
Figure 16: Sampling an artificial object (bottom right) by point clouds generated for scenario 3. Top left: sampling by instrument C. Top right: sampling by instrument B. Bottom left: sampling by instrument A.

Information contained herein is believed to be accurate and reliable.
However, no responsibility is assumed by *RIEGL* for its use.

© Copyright *RIEGL* LMS
page 17 of 21

6 ACQUISITION SPEED

In order to answer the question, "How fast can LIDAR data be acquired with a specific instrument while ensuring a specific sampling quality?", below we provide a plot of the sampling frequency in points/meter, i.e., the inverse of the nominal point spacing versus the acquisition speed measured in square kilometer per hour.

Acquisition speed is simply calculated as the product of ground speed and swath width. Acquisition speed is usually stated in the unit of square kilometers per hour and reflects the area covered by a single swath, not taking into account the commonly used overlap of swaths. We follow the common practice of discarding all measurements lying near the edges of the swath (i.e. near the turning points of the oscillating mirror) for Instruments B and C according to the manufacturers' recommendations.

The figure below shows such a diagram for instrument A. For example, if a sampling frequency over the full swath width of 4 measurements per meter (nominal point spacing of better than 0.25 m) must be achieved, the maximum acquisition speed is 33 km² per hour. The same acquisition speed can be achieved from different heights and different speeds with instrument A within a wide range allowing to adapt to the abilities of the aircraft used. The diagram also reflects the general trend, that acquiring data with a high sampling frequency (low nominal point spacing) asks for a low acquisition speed.
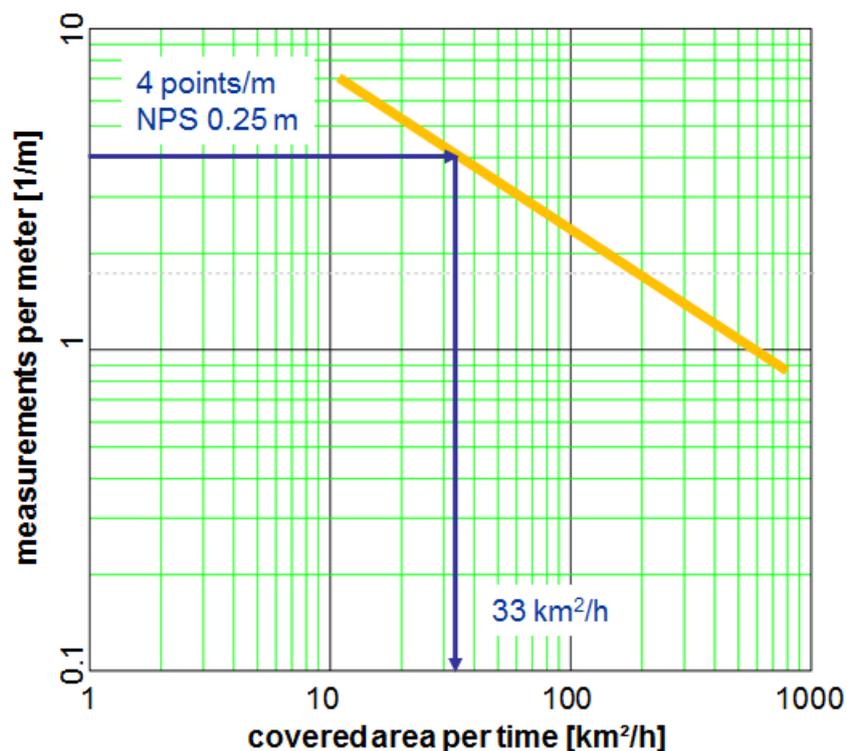
Figure 17: Sampling frequency versus acquisition speed for instrument A. Example on how to read the diagram is shown in blue.

6.1 Comparison of Acquisition Speed for Flat Terrain

In Figure 18 we show the performance as sampling frequency versus acquisition speed for Instrument A and B. For the sake of clarity we do not include the performance of Instrument C in the subsequent diagrams. The performance is slightly worse than that of instrument B.

Information contained herein is believed to be accurate and reliable. However, no responsibility is assumed by *RIEGL* for its use.

© Copyright *RIEGL* LMS
page 18 of 21

In the region from 20 km²/h to 200 km²/h, the difference between Instrument A and B is small. Nevertheless, the 266,000-measurements-per-second system outperforms the 500,000-measurements-per-second system by providing 10% better point spacing and a 20% faster data acquisition. Acquisition speeds above 200 km²/h call for acquisitions from higher heights above ground, which reduces the maximum permitted laser pulse repetition rate for Instrument B as it can only acquire data in a single MTA zone and thus reduces the sampling frequency and acquisition speed even further compared to instrument A. Instrument A outperforms Instrument B in the regime of 600 km²/h by 60% in point spacing and a factor of 2 in acquisition speed. On the left hand side of the diagram, at very high sampling frequencies (more than 4 per meter) the limitations by the oscillating mirror scanner increase the gap in performance in favor of instrument A.
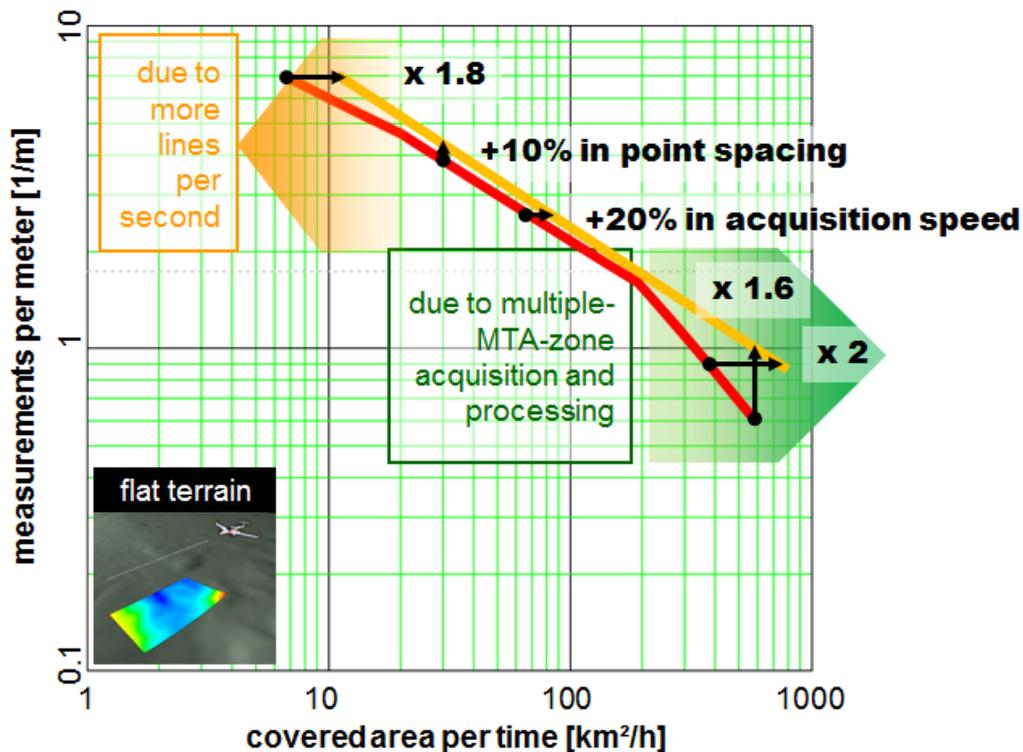

Figure 18: Sampling frequency versus acquisition speed for instruments A (orange) and B (red) for data acquisition on flat terrain. See text for additional explanation on the difference in performance.

6.2   Comparison of Acquisition Speed for Hilly Terrain

For hilly terrain with an assumed variation in height above ground of 200 m within a single strip, the out-of-phase condition between the two channels of Instrument B and C cannot be maintained over the full swath and thus parameters must be optimized differently compared to what has been stated in section 2.4 ($a = b/2$ instead of $a = b$).

Figure 19 shows the performance achievable with Instruments A and B again. The difference is much larger. Even for medium acquisition speeds (20 km²/h to 200 km²/h), data acquisition with Instrument A is 2.6 times faster than Instrument B. Or, for the same acquisition speed, Instrument A provides 60% better sampling frequency.

Information contained herein is believed to be accurate and reliable.
However, no responsibility is assumed by *RIEGL* for its use.

© Copyright *RIEGL* LMS
page 19 of 21

6.3 Comparison of Acquisition Speed for Mountainous Terrain

For mountainous terrain with an assumed variation in height above ground of 1000 m within a single strip, once more the out-of-phase condition between the two channels of Instrument B and C cannot be maintained over the full swath and thus parameters must once again be optimized, this time according to $a = b/2$ instead of $a = b$. Additionally, the restriction that Instrument B can acquire data only in a single preselected MTA zone reduces the permitted laser pulse repetition rate drastically.

Figure 20 shows the performance achievable with Instruments A and B. The difference is significant, both in acquisition speed and in sampling frequency. Even for medium acquisition speeds (20 km²/h to 200 km²/h), data can be acquired with instrument A 8 times faster compared to instrument B. Or, for the same acquisition speed, Instrument A will haves 170 % better sampling frequency. For deriving the diagram we have assumed that no terrain following is used and the trajectories are chosen at fixed altitudes. With Instrument B and C, to ensure a certain sampling quality, terrain following might improve the sampling quality, however, acquisition time and especially acquisition costs will not improve.
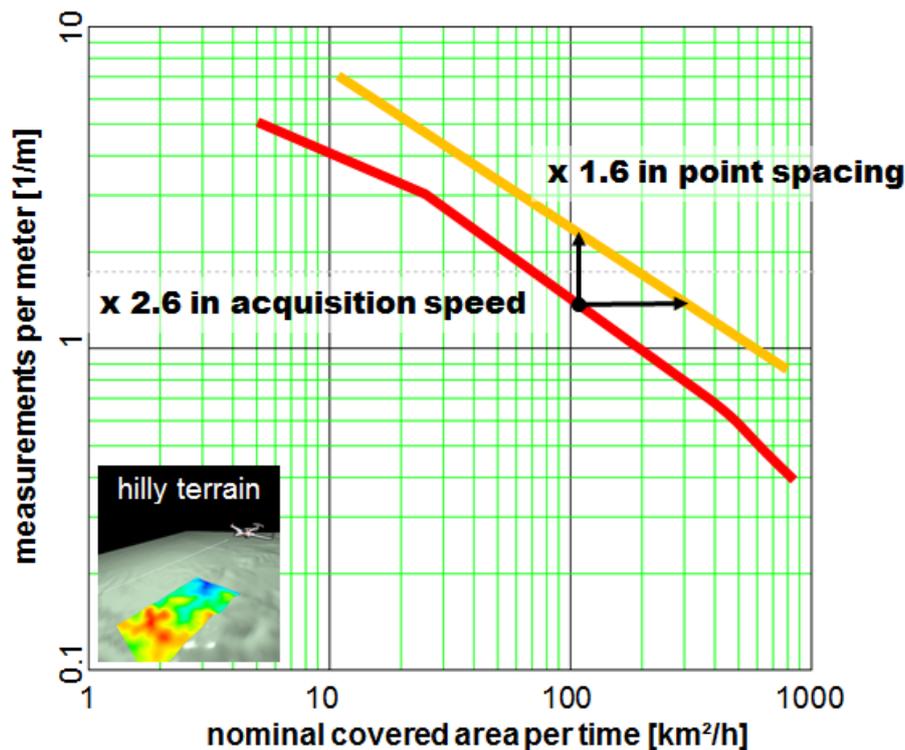

Figure 19: Sampling frequency versus acquisition speed for Instruments A (orange) and B (red) for data acquisition on hilly terrain. See text for additional explanation on the difference in performance.
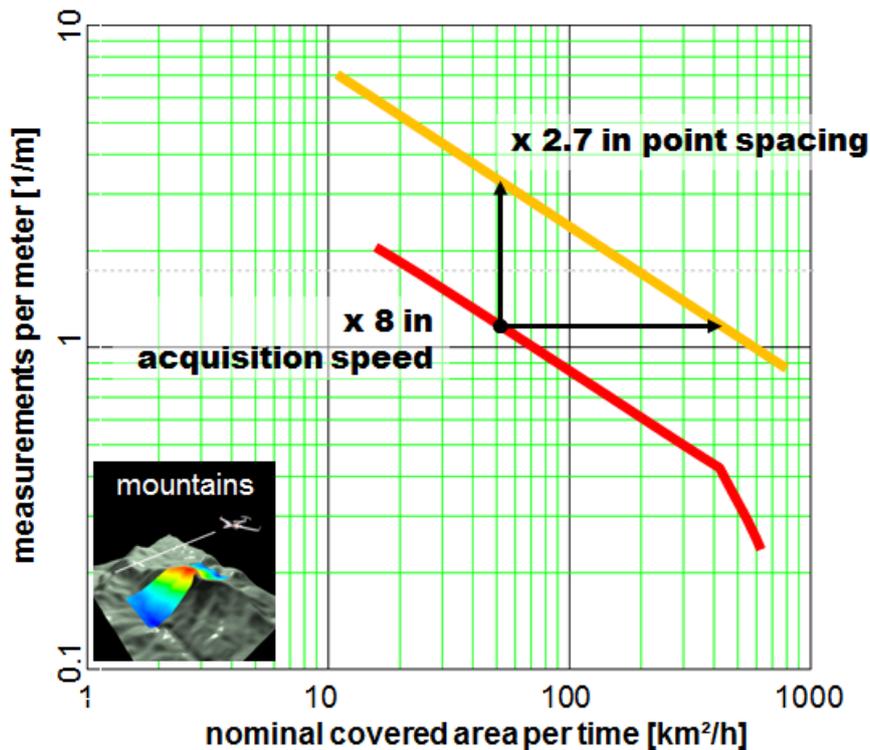
Figure 20: Sampling frequency versus acquisition speed for Instruments A (orange) and B (red) for data acquisition on mountainous terrain. See text for additional explanation on the difference in performance.

7   REFERENCES

[1], Geo-matching, http://www.geo-matching.com, information retrieved February 2013.

[2], Instrument data retrieved from the manufacturer's web sites (in alphabetical order), www.leica-geosystems.com, www.optech.ca, www.riegl.com, all accessed in February 2013

[3], "LIDAR Guidelines and Base Specification", U.S. Geological Survey, National Geospatial Program, Version 13, retrieved from lidar.cr.usgs.gov in January 2013.

[4], "LIDAR density and spacing specification", ASPRS standard Version 1.0, Draft 2.

[5], "Unbiased LIDAR Data Measurements (Draft)", Ty Naus, Fugro Horizon Inc., retrieved from www.asprs.org in January 2013.